Optical surfacing process optimization using parametric smoothing model for mid-to-high spatial frequency error control

Dae Wook Kim[*a], Hubert M. Martin[b] and James H. Burge[a,b]

[a] College of Optical Sciences, University of Arizona, Tucson, Arizona 85721, USA
[b] Steward Observatory, University of Arizona, Tucson, Arizona 85721, USA

* letter2dwk@hotmail.com

ABSTRACT

High performance optical systems aiming for very low background noise from scattering or a sharp point spread function with high encircled energy often specify their beam wavefront quality in terms of a structure function or power spectral density function, which requires a control of mid-to-high spatial frequency surface errors during the optics manufacturing process. Especially for fabrication of large aspheric optics, achieving the required surface figure irregularities over the mid-to-high spatial frequency range becomes a challenging task as the polishing lap needs to be compliant enough to conform to the varying local surface shapes under the lap. This compliance degrades the lap's smoothing capability, which relies on its rigidity. The smoothing effect corrects the mid-to-high spatial frequency errors as a polishing lap removes low spatial frequency (i.e. larger than the lap size) errors on the optical surface. Using a parametric smoothing model developed to quantitatively describe the smoothing effects during Computer Controlled Optical Surfacing (CCOS) processes, actual CCOS data from large aspheric optics fabrication projects have been analyzed and studied. The measured surface error maps were processed with the model to compare different polishing runs using various polishing parameters. The results showing the smoothing effects of mid-to-high spatial frequency surface irregularity will be presented to provide some insights for a CCOS process optimization in terms of smoothing efficiency.

Keywords: Smoothing, computer controlled optical surfacing, mid-to-high spatial frequency error control

1. INTRODUCTION

Many advanced precision optical components such as extremely large astronomical telescope mirrors [1-3] and super smooth lenses for high power laser applications [4] have been manufactured by leveraging dramatic developments in Computer Controlled Optical Surfacing (CCOS) technology since the 1960s [5-9]. The CCOS process, in general, enables highly deterministic figuring process to produce various types of optics such as free-form optics, off-axis aspheric mirrors and anamorphic lenses with superior optical quality.

The Tool Influence Function (TIF), which represents the material removal distribution under a polishing tool with stroke, has been studied for various CCOS processes [7-10] as it is the key to achieving the deterministic capability by accumulating stable TIFs to create a removal distribution matching a target error map. Most TIFs are well modeled using Preston's equation with other advanced models such as parametric edge removal model [11].

Modern high performance optics often require tight specification in terms of mid-to-high spatial frequency errors [3, 12]. For instance, a high performance optical systems (e.g. 8.4m Giant Magellan Telescope primary segment, 8.4m Large Synoptic Survey Telescope (LSST) monolithic primary-tertiary mirror, and 4.2m Advanced Technology Solar Telescope off-axis primary in Fig. 1) aiming for very low background noise from scattering or a sharp point spread function with high encircled energy often specify their optical quality in terms of a structure function, bidirectional reflectance distribution function (BRDF) or power spectral density (PSD) function [3, 12, 13], which requires a tight control of mid-to-high spatial frequency errors during the optical fabrication process.

Optifab 2013, edited by Julie L. Bentley, Matthias Pfaff, Proc. of SPIE Vol. 8884, 88840B
 · doi: 10.1117/12.2028816

Figure 1. 4.2m diameter Advanced Technology Solar Telescope (ATST) off-axis primary Zerodur workpiece, which has a tight bidirectional reflectance distribution function (BRDF) specification to suppress the light scattering from the mirror surface, during the mirror flipping operation in the Optical Engineering and Fabrication Facility (OEFF) at the University of Arizona

While a good conforming characteristic from a polishing tool is required to fabricate free-form or aspheric optics, some rigidity in a tool is also highly desired to get smoothing effects. As shown in Fig. 2 (left) an infinitely rigid tool does not fit to the mid-to-high spatial frequency surface irregularities, and only sits on the high peaks of the optical surface. As the tool moves on the surface in order to achieve a desired removal by targeting errors larger than the size of the tool (i.e. figuring), the mid-to-high spatial frequency errors smaller than the tool size are desired to be smoothed out as shown in Fig. 2 (right). This smoothing effect is a convenient, passive and automatic process to achieve super smooth optical surface efficiently. However, the smoothing effect is not simple to model, evaluate and predict quantitatively, as desired to achieve rapid convergence during the CCOS process.

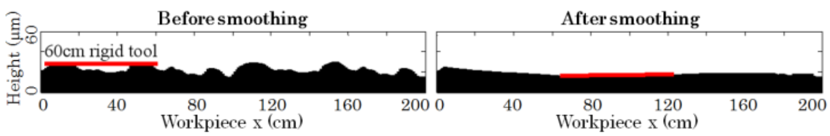

Figure 2. A schematic diagram showing the smoothing effect using an infinitely rigid tool [14]

A generalized parametric smoothing model eliminating the “sinusoidal error analysis only” limit of the previous model [14] was recently developed [15] to process and study the smoothing effects in actual CCOS data. Measured surface maps of the LSST mirror were processed using the new model, and the quantitative smoothing evaluation based on the data has been performed. The results showing the improvements of mid-to-high spatial frequency surface irregularity are presented. A brief review of the parametric smoothing model is given in Section 2, and the analyzed LSST smoothing results are presented in Section 3. Section 4 concludes the discussion.

2. PARAMETRIC SMOOTHING MODEL

Since a smoothing model for an elastic backed lapping belt was introduced by Brown and Parks in 1981 [16] some other meaningful studies have been carried by Jones (smoothing effect of a pitch tool) [17], Mehta and Reid (bridging model for the smoothing effect of a flexible tool) [18] and Tuell (bridging model via a Fourier decomposition approach) [19]. Kim et al. developed the original parametric smoothing model in 2010 to quantify the smoothing efficiency of various polishing processes, but its application is limited to the experimental sinusoidal error cases [14]. A generalized parametric smoothing model to analyze typical surfaces that have a more random topology has been developed in 2013 [15].

The parametric smoothing model simplifies the data processing and provides a quantitative assessment of the surface improvement due to the smoothing effects during an actual CCOS run. The new generalized parametric model defines a smoothing factor SF to describe the smoothing efficiency, which was defined as $\Delta\varepsilon / \Delta z$, where $\Delta\varepsilon$ is the difference between Root-Mean-Square (RMS) values of the local surface errors before and after the smoothing run, and Δz is the nominal removal depth in the local area [15]. The smoothing factor depends on the initial surface error ε_{ini} and that dependence can be parameterized as

$$SF = k \cdot (\varepsilon_{ini} - \varepsilon_0) \tag{1}$$

where k is the sensitivity to the initial error and ε_0 is the minimum error for which smoothing can happen [14, 15]. The smoothing capability of a CCOS process has linear dependence on ε_{ini}. The two parameters k and ε_0 are determined by processing the measured surface error maps before and after a CCOS run with the generalized parametric smoothing model.

3. SMOOTHING RESULT ANALYSIS

3.1 CCOS Run on 8.4m LSST Mirror

The 8.4m LSST workpiece is a monolithic primary-tertiary mirror (primary on outside and tertiary on inside) as shown in Fig. 3. Two fraternal twin tools, stressed lap and RC (Rigid Conformal) lap, were used on each optical surface. They look very different from each other and rely on two radically different concepts (active control [6] vs. passive flow [9]), but eventually provide same functionality (fitting to the aspheric surface under the tool). A computer controlled stressed lap, which actively alters its polishing interface shape to fit the aspheric optical surface, was configured with polyurethane polishing pads on pitch tiles and used to fabricate the LSST primary mirror. The RC lap utilizing a non-Newtonian fluid [9] was used to fabricate the LSST tertiary mirror surface.

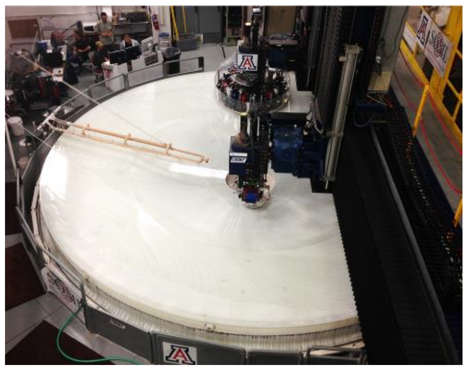

Figure 3. 8.4m diameter Large Synoptic Survey Telescope monolithic primary-tertiary mirror (primary on outside and tertiary on inside) under the large polishing machine equipped with the fraternal twin polishing tools, the stressed lap (top in the picture) and the RC (Rigid Conformal) lap (middle in the picture) in the Steward Observatory Mirror Laboratory at the University of Arizona.

Detailed CCOS parameters for the polishing runs analyzed, including some key dimensions such as tool size and tool interface with workpiece, are summarized and presented in Table 1. For the surface measurements, both interferometric and SCOTS (Software Configurable Optical Test System) measurements were utilized together [20].

Table 1. CCOS parameters for the LSST polishing runs analyzed in Section 3.2

Project	**LSST monolithic primary-tertiary mirror**	
Polishing compound	Zirox K	
Metrology	Interferometer using Computer Generated Hologram and/or Software Configurable Optical Test System [20]	
Polishing tool type	250mm diameter Rigid Conformal lap	800mm diameter Stressed lap
Workpiece outer diameter	5.0m (for tertiary)	8.4m (for primary)
CCOS figuring mode	Dwell time variation mode with fixed 0.6psi polishing pressure	Polishing pressure variation mode with 81 hours total uniform dwell time
Tool interface with workpiece	LP-66 polyurethane pad	LP-66 polyurethane pad on pitch

3.2 Smoothing Results

Two sets of measured surface error maps from both cases described in Table 1 were processed using the generalized parametric smoothing model. The initial surface maps for the primary with 866nm RMS target error (left) and the tertiary with 192nm RMS (right) target error are shown in Fig. 4. However, it is important to note that the smoothing results presented in this study are the mid-to-high spatial frequency errors smaller than the tool size [12-15]. Instead of simply monitoring the overall surface RMS value changes before and after the CCOS run, which represents a figuring (in contrast to smoothing) efficiency, all the local areas (smaller than the tool size) in the surface maps are independently analyzed via the smoothing model [15]. As a reference, the relative tool (contact area) size is depicted as a black disk in the bottom-right corner of the surface error maps in Fig. 4.

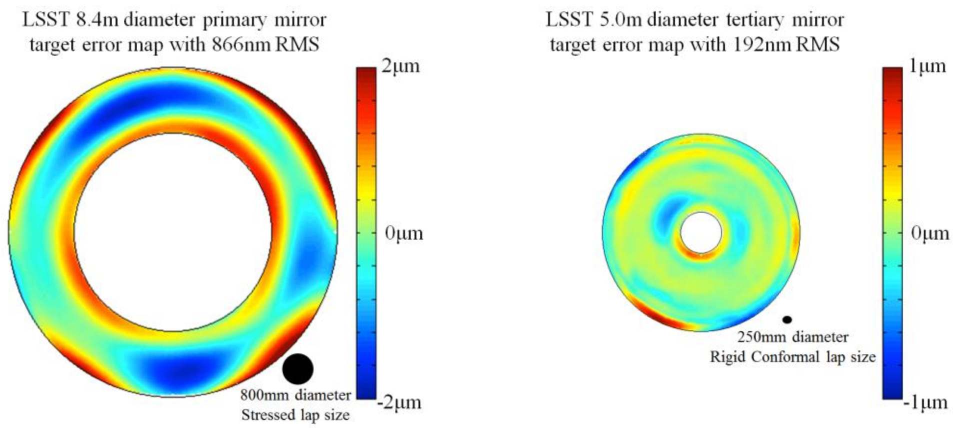

Figure 4. LSST primary (left) and tertiary (right) mirror surface error map before the CCOS runs, which were used as the target removal maps during the runs. The relative tool (contact area) size is depicted as a black disk in the bottom-corner.

The processed smoothing factor *SF* values as a function of initial local (not overall) surface error ε_{ini} are plotted in Fig. 5. The 800mm stressed lap with LP-66 on pitch tiles showed about 10-20% higher *SF* values for most initial local surface RMS error ε_{ini} range than the 250mm RC lap with same polyurethane pads. However, overall, the differences between the two cases are within 1σ (standard deviation) range.

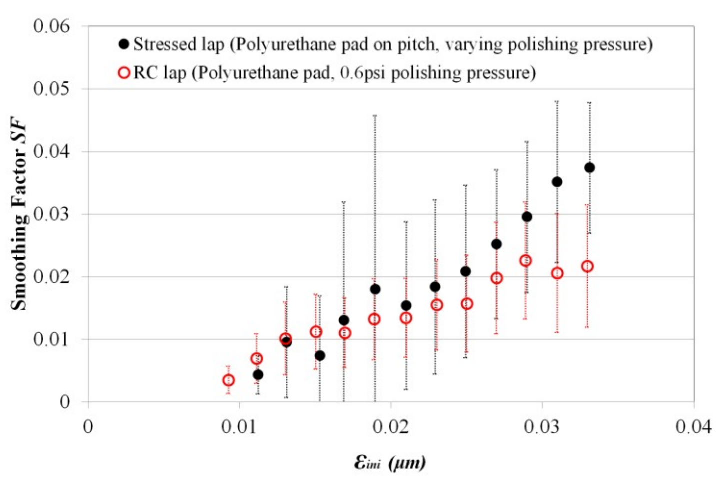

Figure 5. Smoothing efficiency comparison: *SF* vs. ε_{ini} (initial local surface RMS error) for 800mm stressed lap with polyurethane pads on pitch tiles (black solid circle) and 250mm RC lap with polyurethane pad (red open circle). (The bar represents the spread (+/- 1σ, standard deviation) of the *SF* values.)

We acknowledge that these two case study results presented here are not enough to draw some general conclusions as there might be various other parameters affecting the *SF* calculations. (More rigorous statistical study to compare various smoothing factor results all together is currently being planned as more actual CCOS data will be processed using the generalized smoothing model.) However, the result in Fig. 5 gives very useful knowledge that the large stressed lap with polyurethane pads on pitch tiles has slightly better smoothing efficiency than the RC lap. The fact that two tools with very different structures, but a common polyurethane polishing interface, have similar smoothing efficiency supports the hypothesis that the smoothing efficiency is mainly limited by the polyurethane pad's characteristics (e.g. stiffness) not by the backing materials (e.g. pitch tile vs. visco-elastic non-Newtonian fluid). Other tests, including comparison of bare pitch and pitch faced with polyurethane, support the same conclusion.

This quantitative smoothing evaluation for two different types of tools provides some useful insights to optimize and improve the smoothing efficiency of current CCOS process. For instance, the stressed lap might need to be used without the polyurethane pads on pitch tiles in order to maximize its smoothing effects. Also, for the RC lap, some changes in the polishing interface material (LP-66 at the moment) may result in a noticeable improvement in terms of the *SF* slope *k*, which is directly related to the tool's mid-to-high spatial frequency error control capability.

4. CONCLUSION

High performance optical systems aiming for very low background noise from scattering or a sharp point spread function often specify their beam wavefront quality in terms of a structure function or power spectral density function. The smoothing effect provides a highly efficient and convenient way to correct mid-to-high spatial frequency errors as a polishing lap removes low spatial frequency errors on the optical surface. Using the new generalized parametric smoothing model, which provides a systematic way to evaluate the smoothing effects, actual surface measurement data from the LSST monolithic primary-tertiary mirror fabrication project have been analyzed and studied. The results showed the smoothing effects of mid-to-high spatial frequency surface irregularity for the two different types of polishing tools, stressed lap and RC lap. These results give an objective evaluation of the current CCOS process in terms of smoothing and provide a valuable guide toward further improvements in smoothing efficiency for CCOS processes.

REFERENCES

[1] R. Angel, "Very large ground-based telescopes for optical and IR astronomy 4", Nature **295**, 651-657 (1982).

[2] R. Angel, "Future optical and infrared telescopes 3", Nature **409**, 427-430 (2001).

[3] H. M. Martin, R. G. Allen, J. H. Burge, D. W. Kim, J. S. Kingsley, K. Law, R. D. Lutz, P. A. Strittmatter, P. Su, M. T. Tuell, S. C. West and P. Zhou, "Production of 8.4 m segments for the Giant Magellan Telescope," Proc. SPIE **8450** (2012).

[4] J. H. Campbell, R. A. Hawley-Fedder, C. J. Stolz, J. A. Menapace, M. R. Borden, P. K. Whitman, J. Yu, M. Runkel, M. O. Riley, M. D. Feit and R. P. Hackel, "NIF optical material and fabrication technologies: An overview", Proc. SPIE **5341**, p.84-101, (2004).

[5] R A. Jones, "Computer control for grinding and polishing," Photon. Spectra, 34-39 (1963).

[6] S. C. West, H. M. Martin, R. H. Nagel, R. S. Young, W. B. Davison, T. J. Trebisky, S. T. DeRigne and B. B. Hille, "Practical design and performance of the stressed-lap polishing tool" Appl. Opt. **33**, 8094-8100, (1994).

[7] D. Golini, W. I. Kordonski, P. Dumas and S. Hogan, "Magnetorheological finishing (MRF) in commercial precision optics manufacturing", Proc. SPIE **3782**, p.80-91, (1999).

[8] D. D. Walker, R. Freeman, R. Morton, G. McCavana and A. Beaucamp, "Use of the 'Precessions'™ process for prepolishing and correcting 2D & 2½D form," Opt. Express **14**, 11787-11795 (2006).

[9] D.W. Kim and J. H. Burge, "Rigid conformal polishing tool using non-linear visco-elastic effect," Opt. Express **18**, 2242-2257 (2010).

[10] D. W. Kim, S. W. Kim and J. H. Burge, "Non-sequential optimization technique for a computer controlled optical surfacing process using multiple tool influence functions," Opt. Express **17**(24), 21850–21866 (2009).

[11] D. W. Kim, W. H. Park, S. W. Kim, and J. H. Burge, "Parametric modeling of edge effects for polishing tool influence functions," Opt. Express. **17**, 5656-5665 (2009).

[12] D. W. Kim, H. M. and J. H. Burge, "Control of Mid-spatial-frequency Errors for Large Steep Aspheric Surfaces," in Optical Fabrication and Testing (OF&T) Technical Digest (Optical Society of America, Washington, DC), OM4D.1 (2012).

[13] J. D. Hoyo, D. W. Kim and J. H. Burge, "Super-smooth optical fabrication controlling high-spatial frequency surface irregularity," Proc. SPIE **8838**, 88380T (2013).

[14] D. W. Kim, Won Hyun Park, Hyun Kyoung An and J. H. Burge, "Parametric smoothing model for visco-elastic polishing tools," Opt. Express **18**, 22515-22526 (2010).

[15] Y. Shu, D. W. Kim, H. M. Martin and J. H. Burge, “Correlation-based smoothing model for optical polishing,” submitted to Optics Express.
[16] N. J. Brown and R. E. Parks, “The polishing-to-figuring transition in turned optics,” SPIE’s 25th Annual International Technical Symposium, (SPIE, 1981).
[17] R. A. Jones, “Computer simulation of smoothing during computer-controlled optical polishing,” Appl. Opt. **34**, 1162-1169 (1995).
[18] P. K. Mehta and P. B. Reid, “A mathematical model for optical smoothing prediction of high-spatial frequency surface errors,” Proc. SPIE **3786**, 447 (1999).
[19] M. T. Tuell, “Novel tooling for production of aspheric surfaces,” M.S. Thesis (2002).
[20] P. Su, R. E. Parks, L. Wang, R. P. Angel and J. H. Burge, “Software configurable optical test system: a computerized reverse Hartmann test.” Appl. Opt. **49**, 4404-4412 (2010).

ACKNOWLEDGEMENTS

LSST project activities are supported in part by the National Science Foundation through Governing Cooperative Agreement 0809409 managed by AURA, and the Department of Energy under contract DE-AC02-76-SFO0515 with the SLAC National Accelerator Laboratory. Additional LSST funding comes from private donations, grants to universities, and in-kind support from LSSTC Institutional Members. In addition, this material is based in part upon work performed for the Advance Technology Solar Telescope (ATST). The ATST is managed by the National Solar Observatory (NSO), which is operated by the Association of Universities for Research in Astronomy, Inc. (AURA) under a cooperative agreement with the National Science Foundation (NSF).